Polymers **2014**, *6*, 2232-2246; doi:10.3390/polym6082232

OPEN ACCESS

polymers

ISSN 2073-4360

www.mdpi.com/journal/polymers

Article

Effects of Graphene Nanoplatelets and Reduced Graphene Oxide on Poly(lactic acid) and Plasticized Poly(lactic acid): A Comparative Study

Buong Woei Chieng [1,*], Nor Azowa Ibrahim [1], Wan Md Zin Wan Yunus [2], Mohd Zobir Hussein [3], Yoon Yee Then [1] and Yuet Ying Loo [4]

[1] Department of Chemistry, Faculty of Science, Universiti Putra Malaysia, 43400 UPM Serdang, Selangor, Malaysia; E-Mails: norazowa@upm.edu.my (N.A.I.); yoonyeetyy84@yahoo.com (Y.Y.T.)

[2] Department of Chemistry, Centre for Defence Foundation Studies, National Defence University of Malaysia, Sungai Besi Camp, 57000 Kuala Lumpur, Malaysia; E-Mail: wanmdzin@upnm.edu.my

[3] Materials Synthesis and Characterization Laboratory, Institute of Advanced Techonology, Universiti Putra Malaysia, 43400 UPM Serdang, Selangor, Malaysia; E-Mail: mzobir@upm.edu.my

[4] Department of Food Science, Faculty of Food Science and Technology, Universiti Putra Malaysia, 43400 UPM Serdang, Selangor, Malaysia; E-Mail: yuet_ying88@hotmail.com

* Author to whom correspondence should be addressed; E-Mail: chieng891@gmail.com; Tel.: +603-8946-6802; Fax: +603-8943-2508.

Received: 13 June 2014; in revised form: 24 July 2014 / Accepted: 25 July 2014 / Published: 21 August 2014

Abstract: The superlative mechanical properties of graphene-based materials make them the ideal filler materials for polymer composites reinforcement. Two types of graphene-based materials, graphene nanoplatelets (xGnP) and reduced graphene oxide (rGO), were used as nanofiller in poly(lactic acid) (PLA) polymer matrix, as well as plasticized PLA. The addition of rGO into PLA or plasticized PLA substantially enhanced the tensile strength without deteriorating elasticity, compared to xGnP nanocomposites. In addition, the investigation of the thermal properties has found that the presence of rGO in the system is very beneficial for improving thermal stability of the PLA or plasticized PLA. Scanning electron microscope (SEM) images of the rGO nanocomposites display homogenous and good uniformity morphology. Transmission electron microscopy (TEM) images revealed that the rGO remained intact as graphene sheet layers and were dispersed

well into the polymer matrix, and it was confirmed by X-ray diffraction (XRD) results, which shows no graphitic peak in the XRD pattern.

Keywords: graphene nanoplatelets; reduced graphene oxide; plasticized; poly(lactic acid)

1. Introduction

The discovery of new nano-material graphene by Andre Geim in 2004 [1], attracted worldwide interest among researchers. Graphenes have generated huge activities in most areas of science and engineering due to their unprecedented physical and chemical properties. Graphene, which is fabricated from natural graphite, can be used as a potential alternative nano-reinforcement element to both clays and carbon nanotubes, which can then provide excellent functional properties enhancements [2]. There are a number of reasons for producing graphene-based polymer nanocomposites. The addition of a filler with such impressive mechanical properties is expected to lead to a significant improvement in the mechanical properties of the host polymer matrix [3,4].

Poly(lactic acid) (PLA) has received great attention in the scientific community recently due to its biodegradability and its origin which is based on natural resources [5]. PLA offers a possible alternative to the traditional non-biodegradable polymers such as polyethylene and polypropylene especially when recycling them is difficult or not economical. However, some of its disadvantages, such as relatively poor mechanical properties and gas barrier, slow crystallization rate and low thermal stability, have limited its wider applications [6]. Therefore, polymer blending and preparation of nanocomposites have often been employed to modify the physical properties of PLA in order to extend the practical applications [7–11]. Various nano-reinforcement fillers, such as layered silicate clay [12], carbon nanotubes [13], and layered double hydroxide [14], are being developed and extensively studied in various polymer matrices.

Graphene Nanoplatelets (xGnP) are a new class of filler which consist of small stacks of graphene and are usually 1–15 nm thick. xGnPs are prepared by intercalating graphite either with metal ions or by acid treatment, which is then further exfoliated via thermal treatment. It has a similar layered structure compared to clay, but with better mechanical properties. Thus, xGnP is shown as a promising material used as filler in polymer nanocomposites. Nevertheless, the properties enhancement in polymer nanocompoistes strongly depends on the number of layers stacked in xGnPs, the degree of crystallinity in the graphitic plane, their aspect ratio, and the order of staking [15].

Oxidative exfoliation of natural graphite by thermal or oxidation technique and subsequent chemical reduction has been known as the most efficient and low cost method to produce graphene or more likely to called as reduced graphene oxide (rGO). In principle, it would be expected that the incorporation of rGO would lead to a stronger reinforcement effect than the incorporation of Graphene Nanoplatelets (xGnP), considering that the rGO exist in an exfoliated individual graphene sheets which had an even higher aspect ratio than xGnP. There are many studies on graphene composites based on a range of polymers available in literature, e.g., polycarbonate [16], Nylon [17], poly(methyl methacrylate) [18], poly(vinylidene fluoride), epoxy [19], poly(vinyl alcohol) [20], polystyrene [21], poly(ethylene disulfide) [22], poly(propylene) [23], poly(lactic acid) [24,25], *etc*. An investigation on the mechanical aspects of

epoxy/xGnP by Chanrasekaran *et al.* [19] showed that effective mechanical reinforcement was achieved for 0.5 wt% with 17% increase in glassy storage modulus. A considerable increase in fracture toughness of 43% was obtained for 1.0 wt% of filler loading. In another study on epoxy/xGnP composite at low filler content of 0.1 wt%, a noticeable increment of 31% in modulus and 40% in fracture toughness was observed [26]. Recently, Inuwa *et al.* [27] prepared xGnP reinforced Poly(ethylene terephthalate) (PET)/PP composites by melt blending method. The maximum flexural strength and impact strength of the composites were obtained at 3 phr xGnP loading. The composites have significantly enhanced thermal stability with the highest stability at 3 phr loading.

In this study, reduced graphene oxide (rGO) was used as nanofiller in PLA polymer matrix, as well as epoxidized palm oil (EPO)-plasticized PLA and poly(ethylene glycol) (PEG)-plasticized PLA. The result of rGO nanocomposites were compared with xGnP nanocomposites.

2. Experimental Section

2.1. Materials

Poly(lactic acid) (PLA) Natureworks grade 4042D (95.8% L-lactide, 4.2% D-lactide), number average molecular mass, M_n = 183,000 g/mol was purchase from NatureWorks® LLC (Minnetonka, MN, USA). Low molecular weight poly(ethylene glycol) (PEG) (M_n = 200 g/mol) was purchased from Sigma-Aldrich (St. Louis, MO, USA). Epoxidized Palm Oil (EPO) was obtained from pilot plant in Advanced Oleochemical Technology Division (AOTD) of Malaysia Palm Oil Board (MPOB), Selangor, Malaysia. Graphene nanoplatelets, trade name xGnP®, Grade M, was supplied by XG sciences Inc. (Lansing, MI, USA). Each particle consists of several sheet of graphene with an average thickness of approximately 6–8 nm and average diameter of 15 μm. Reduced graphene oxide (rGO) was synthesized by reduction of graphene oxide with average size of 15 μm.

2.2. Preparation of Plasticized PLA/xGnP and Plasticized PLA/rGO Nanocomposites

The PLA-based xGnP and rGO nanocomposites were prepared by melt blending technique using Brabender® internal mixer (GmbH & Co. KG, Duisburg, Germany) with 50 rpm of the rotor speed, at 170 °C for 10 min. EPO and PEG was used as plasticizer to plasticize PLA. The xGnP and rGO content was fixed at 0.3 wt%. The blends obtained were then molded into sheets of 1 mm in thickness by hot pressing at 165 °C for 10 min with pressure of 110 kg/cm^2, followed by cooling to room temperature. The sheets were used for further characterization.

2.3. Characterizations

2.3.1. X-ray Diffraction (XRD)

X-ray diffraction measurement was carried out by using a Shimadzu XRD 6000 X-ray diffractometer (Tokyo, Japan) with CuK_α radiation (λ = 1.542 Å) operated at 30 kV and 30 mA. Data were recorded in 2θ range of 2°–10° at the scan rate of 2°/min.

2.3.2. Fourier Transform Infrared (FTIR)

FTIR spectra were recorded using Fourier Transform Infrared Spectrometer Perkin Elmer BX (Waltham, MA, USA) equipped with a universal attenuated total reflectance. The spectra were recorded between 4000 and 280 cm^{-1} frequency ranges.

2.3.3. Tensile Properties Measurement

Tensile properties test were carried out by using Instron 4302 series IX (Norwood, MA, USA). The samples were cut into dumbbell shape follow ASTM D638 (type V) standard [28]. Load of 1.0 kN was applied at constant crosshead speed of 10 mm/min at room temperature. Tensile strength, tensile modulus and elongation at break were evaluated from the stress-strain data. Each sample included seven tested replicates to obtain a reliable mean and standard deviation.

2.3.4. Thermal Properties

Thermogravimetric analysis (TGA) was carried out using a Perkin Elmer Pyris 7 TGA analyzer (Waltham, MA, USA) with scan range from 35° to 800° at a constant heating rate of 10 °C/min and continuous nitrogen flow. The thermal degradation temperature taking into account were the temperature at onset (T_{onset}), the temperature of maximum weight loss (T_{max}) and temperature at 50% weight loss (T_{50}).

2.3.5. Morphology

The fracture surfaces of tensile failed sample were studied under a JEOL scanning electron microscopy (SEM) instrument JSM-6400 (Tokyo, Japan) at an accelerating voltage of 30 kV. The fractured surfaces were coated with a thin layer of gold prior to observation. Transmission electron microscopy (TEM) image were obtained using a Hitachi H-7100 TEM (Tokyo, Japan) operated at an accelerating voltage of 100 kV to observe the nanocomposites. All samples were ultrathin-sectioned using a microtome equipped with a diamond knife.

3. Results and Discussion

3.1. Fourier Transform Infrared (FTIR)

Figure 1 shows the FTIR spectra of (a) xGnP nanocomposites and (b) rGO nanocomposites respectively in comparison with pristine PLA. The PLA spectrum shows four main regions: –CH stretching at 3000–2850 cm^{-1}, –C=O stretching at 1750–1745 cm^{-1}, C–H bending at 1500–1400 cm^{-1} and –C–O stretching at 1100–1000 cm^{-1}. It should be noted that, the significant characteristic peaks of PLA were still dominant upon addition of both xGnP and rGO. The characteristic peaks responsible for –CH stretching, –C=O stretching, C–H bending, as well as –C–O stretching were clearly observed over the spectra for all nanocomposites and no new peak was formed. Therefore, it could be concluded that there was no chemical interaction with polymer matrices upon addition of xGnP or rGO. This is expected due to xGnP and rGO not having any functional groups available to form strong interface with a polymer matrix.

Therefore, any property change of the nanocomposites is the result of the physical interaction only between the xGnPs and the plasticized PLA matrix. A similar conclusion was arrived at by Inuwa *et al.* [27]. Inuwa *et al.* reported that there was no significant change in peak positions of PET/PP/GnP composites compared to pristine PET/PP blend.

Figure 1. Fourier Transform Infrared (FTIR) of poly(lactic acid) (PLA): (**a**) graphene nanoplatelets (xGnP) nanocomposites; and (**b**) reduced graphene oxide (rGO) nanocomposites.

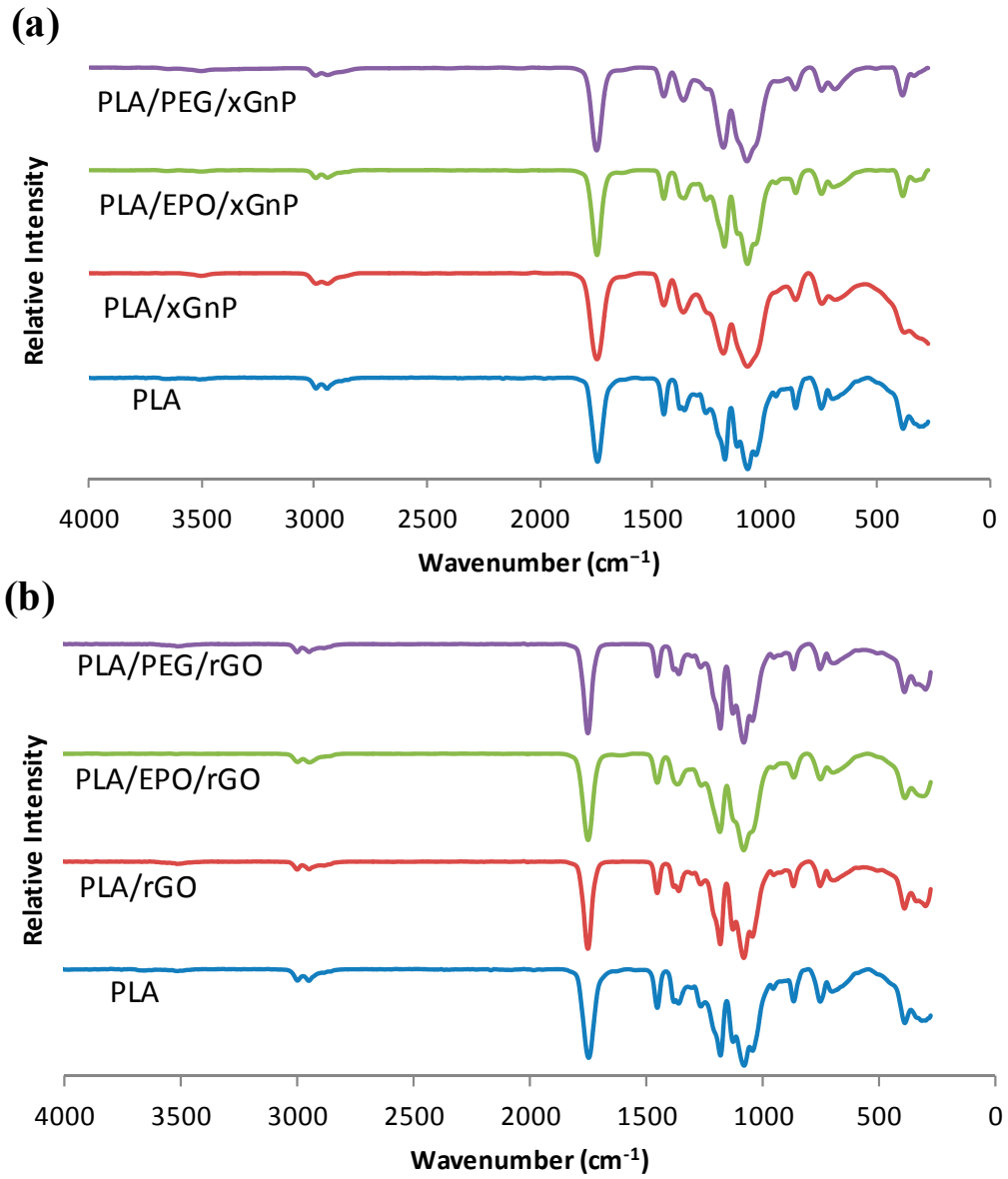

3.2. X-ray Diffraction (XRD)

Figure 2 shows the XRD patterns for xGnP nanocomposites. An exceptionally wide diffraction from 10° to 25° is caused by the scattering of PLA polymer matrix. A sharp diffraction is observed at 26.6°, relating to an interlayer spacing of 0.34 nm based on the Bragg's law, which is associated with graphitic (002) plane. Obviously, there is no marked difference in terms of the (002) diffraction angle at 26.6° for all xGnP nanocomposites. However, this (002) diffraction peak was not observed in rGO nanocomposites, as shown in Figure 3. This attributed to the fully exfoliated graphitic layers of rGO.

Additionally, this graphene layers were not reassembled or re-aggregated when rGO was incorporated in PLA matrix. Thus, the rGO still exists in a single graphene layer and exfoliated in PLA matrix as can be confirmed in TEM images.

Figure 2. X-ray Diffraction (XRD) patterns of PLA, Poly(lactic acid) (PLA)/epoxidized palm oil (EPO), and Poly(lactic acid) (PLA)/poly(ethylene glycol) (PEG) with 0.3 wt% of xGnP.

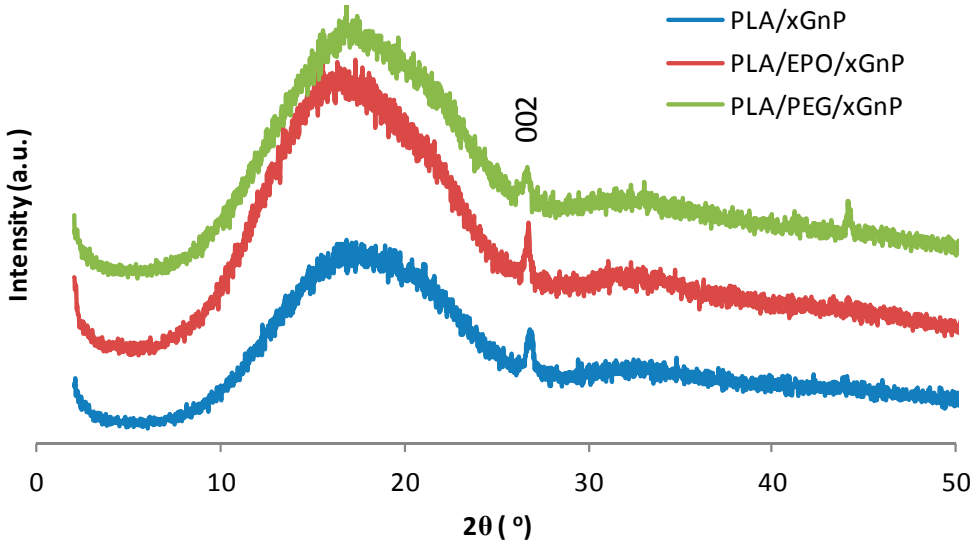

Figure 3. XRD patterns of PLA, PLA/EPO and PLA/PEG with 0.3 wt% of rGO.

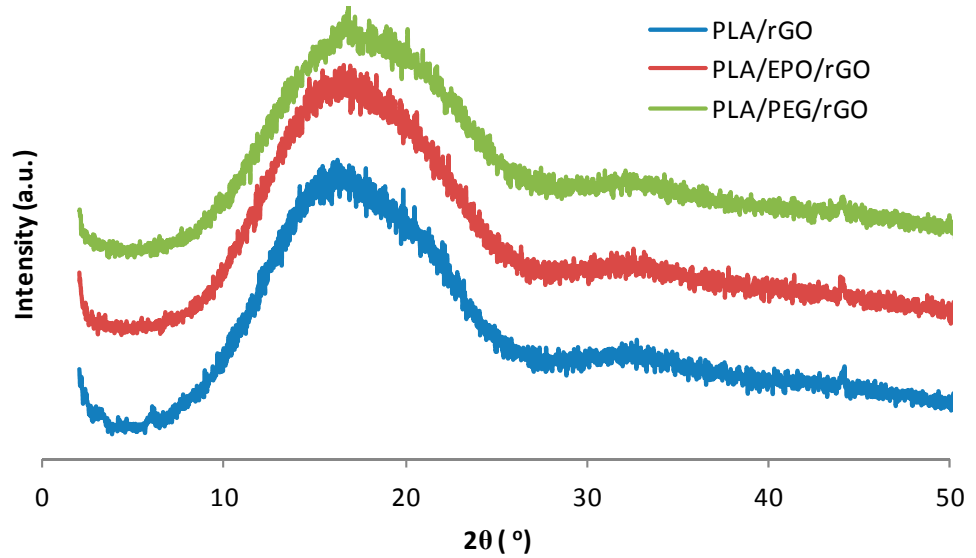

3.3. Tensile Properties

The tensile properties of nanocomposites are significantly affected by the following factors: (I) the dispersiblity of graphene-based nanofillers in PLA matrix; (II) the interfacial interaction between graphene-based nanofillers and PLA matrix; (III) the crystallization behavior of the nanocomposites. However, there was no significant difference in the crystallinity of the PLA/rGO nanocomposites as seen from the XRD patterns (Figures 2 and 3). Thus, the difference of the tensile properties caused by crystallinity might be ignored. From our previous studies in plasticized PLA/xGnP nanocomposites [7,10],

xGnP was effective in achieving improved tensile properties for EPO-plasticized PLA and PEG-plasticized PLA blend. Tensile tests show very significant improvements with the addition of very small amounts of xGnP (<1.0 wt%). An optimum loading is identified of 0.3 wt% xGnP, and this amount was used and compared to rGO in this study. In principle, it would be expected that the incorporation of rGO would lead to a stronger reinforcement effect than the incorporation of xGnP, considering that the rGO exists in an exfoliated individual graphene sheets when dispersed in polymer matrices which had a even higher aspect ratio than xGnP as shown in Figure 4.

Figure 4. Illustration of dispersion of (**a**) xGnP and (**b**) rGO in polymer matrix.

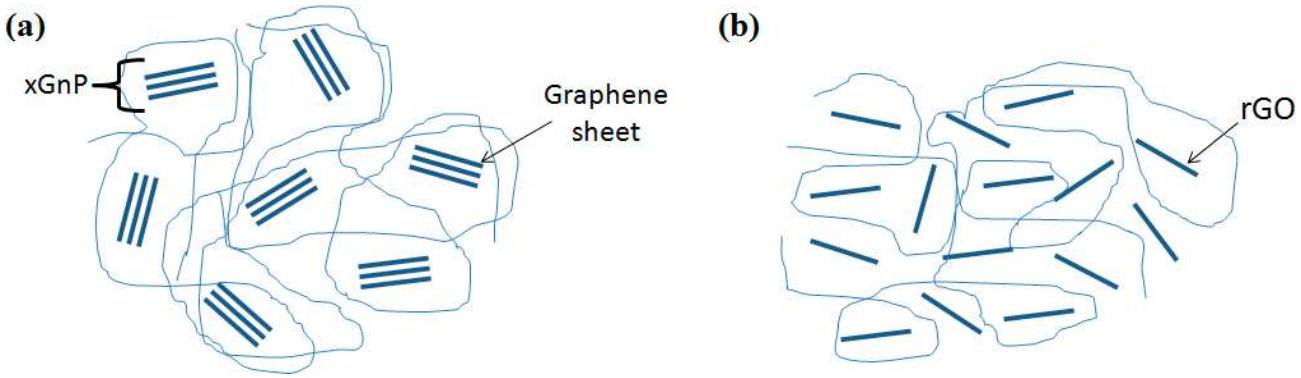

Figure 5 shows the effect of rGO on the tensile strength of PLA and plasticized PLA in comparison with xGnP. Pristine PLA shows a high tensile strength of 57.98 MPa. The addition of both rGO and xGnP into PLA further improved the tensile strength of PLA. When rGO was added into the PLA matrix, the tensile strength of PLA/rGO nanocomposite increased from 60.49 to 62.18 MPa (an increase of 3%) compared to PLA/xGnP. As to PLA/EPO/rGO nanocomposites, tensile strength increased from 41.07 to 42.62 MPa (an increase of 4%). This attributed to higher aspect ratio, better dispersion and interfacial stress transfer of rGO compared to xGnP. Good dispersion and interfacial stress transferring lead to a more uniform stress distribution and minimize the presence of the stress concentration center [29].

Figure 5. Effect of xGnP and rGO on tensile strength of PLA and plasticized PLAs.

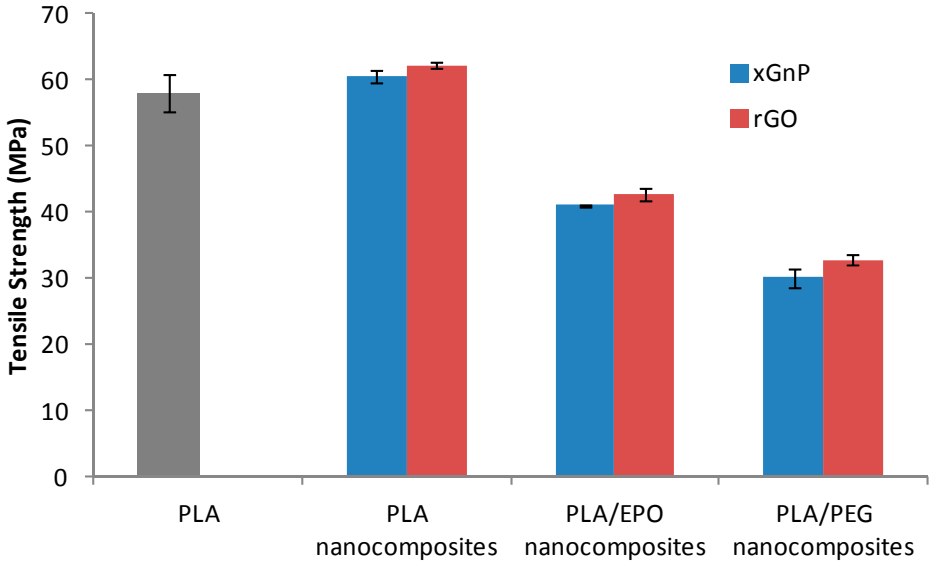

The effect of rGO and xGnP on tensile modulus and elongation at break are shown in Figures 6 and 7, respectively. PLA shows a very high tensile modulus (1136 MPa) and low elongation at break (5.4%) due to its brittle nature. Meanwhile, EPO-plasticized and PEG-plasticized PLA nanocomposites show a lower tensile modulus and high elongation at break due to the plasticizing effect of EPO and PEG plasticizers. The tensile modulus is always inversely proportional to the elongation at break. The rGO has a great impact on elongation at break and tensile modulus compared to xGnP. rGO nanocomposites shows improvement of 261.8%, 53.9% and 5.6% for PLA, PLA/EPO and PLA/PEG, respectively, compared to xGnP filled nanocomposites in elongation at break The improvement in elongation at break indicated the addition of rGO enhanced the toughness of PLA. However, the enhanced toughness caused the decrease of tensile modulus as can see in Figure 6. rGO nanocomposites shows decrement of 11.4%, 42.1% and 22.1% for PLA, PLA/EPO, and PLA/PEG, respectively, compared to xGnP filled nanocomposites in tensile modulus. The reduction in tensile modulus is a trade-off between elongation at break and it remains a great challenge to realize simultaneous strength and toughness improvement.

Figure 6. Effect of xGnP and rGO on tensile modulus of PLA and plasticized PLAs.

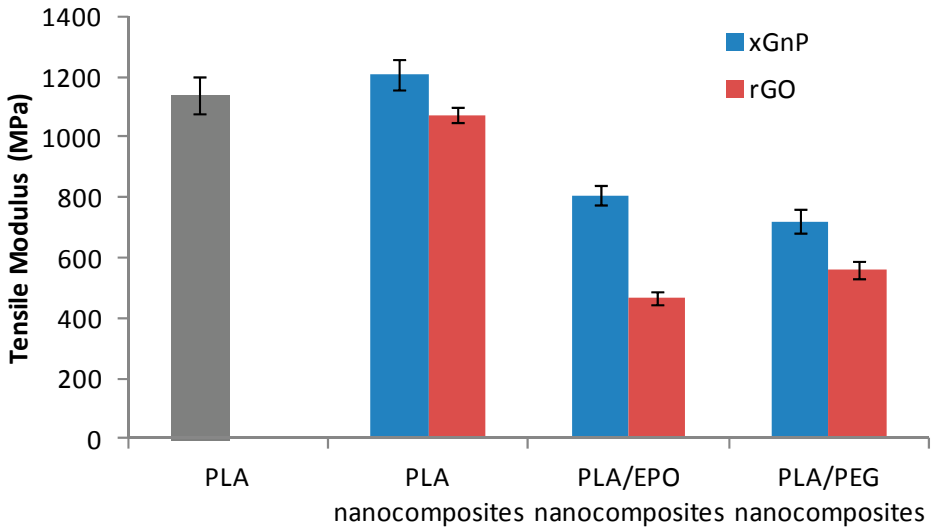

Figure 7. Effect of xGnP and rGO on elongation at break of PLA and plasticized PLAs.

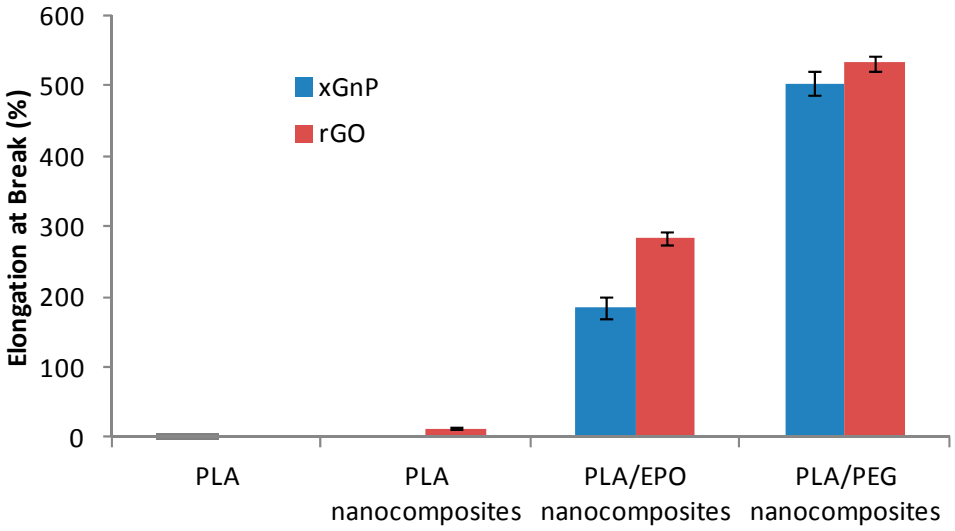

3.4. Thermogravimetric Analysis (TGA)

Thermal stability is an important property for polymer nanocomposites. The TG and DTG curves for xGnP and rGO nanocomposites are illustrated in Figure 8. The characteristic temperatures of xGnP and rGO nanocomposites are tabulated in Table 1 for comparison purposes. The thermal behavior of PLA and its nanocomposites show only one degradation stage. It can be seen that the decomposition temperature of the nanocomposites commences at around 250 °C and rapidly continues until 400 °C. Notice that from the graph, the PLA nanocomposites and EPO-plasticized PLA nanocomposites have a higher thermal stability than pristine PLA. The improved thermal stability in EPO-plasticized PLA nanocomposites is possibly due to an interaction between the hydroxyl group of PLA and the epoxy group of EPO through hydrogen bonding. Meanwhile, the PEG-pasticized PLA nanocomposites show a lower thermal stability compared to pristine PLA. The decrease of the PLA thermal stability is mainly due to the presence of PEG as plasticizer. PEG promotes a decrease in thermal stability by its action to intersperse itself around polymers and by breaking polymer-polymer interaction, which are predicted in the lubricity theory and gel theory of plasticization [30].

Figure 8. Thermogravimetric (TG) thermograms of (**a**) PLA; (**b**) plasticized PLA/EPO; and (**c**) plasticized PLA/PEG nanocomposites.

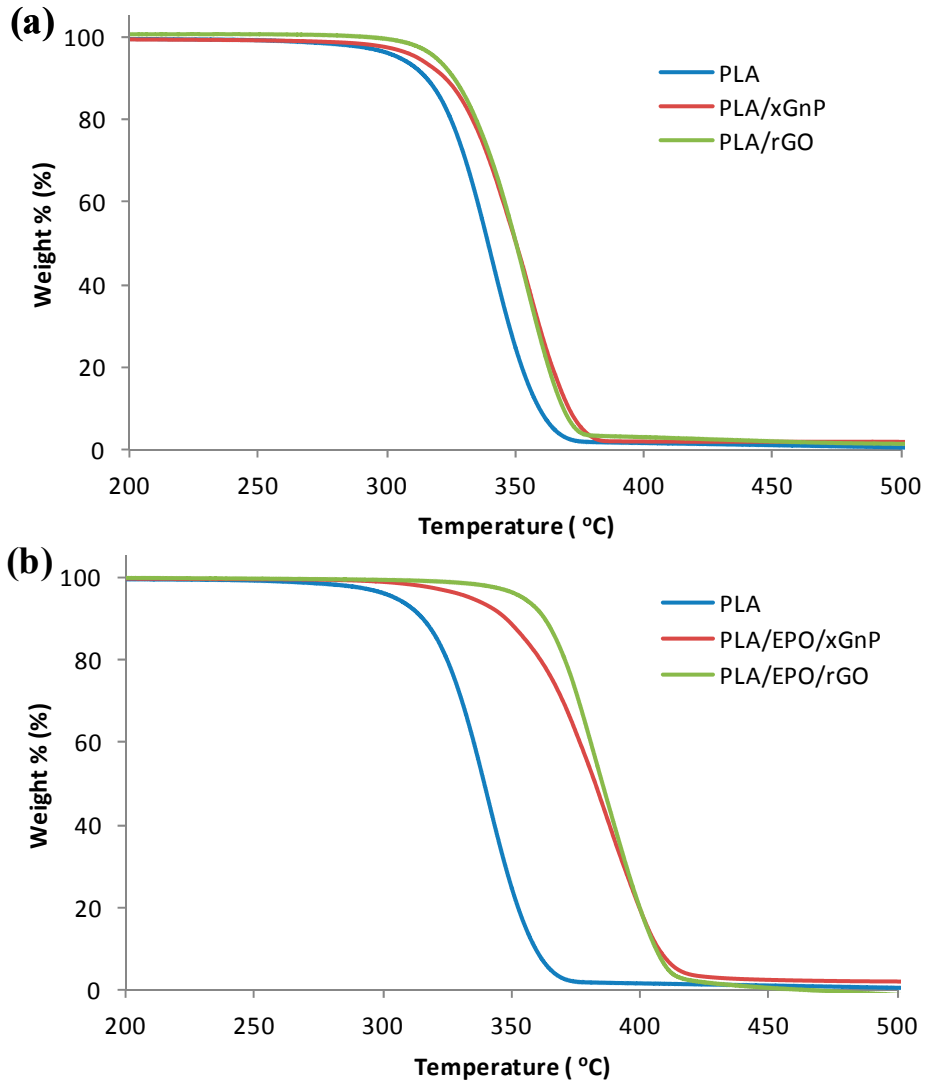

Figure 8. *Cont.*

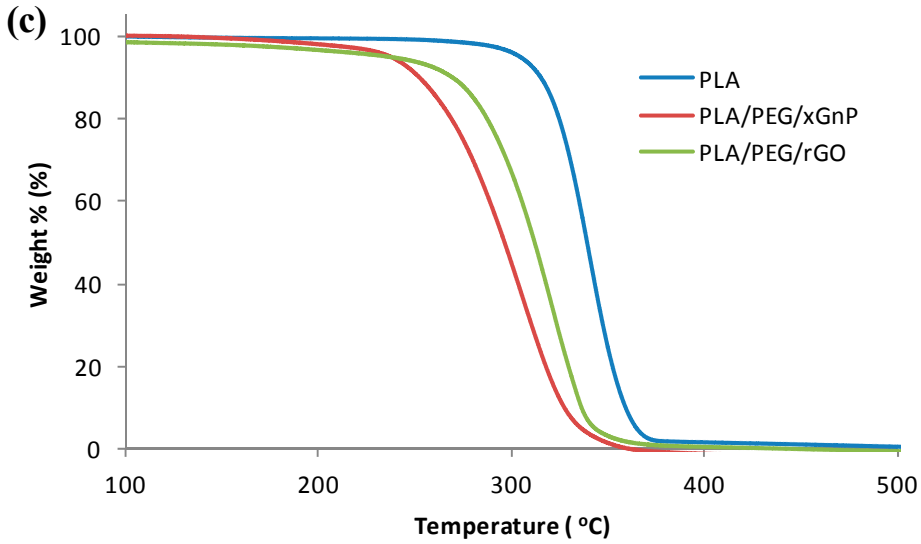

Table 1. Characteristic temperatures of graphene nanoplatelets (xGnP) and reduced graphene oxide (rGO) nanocomposites.

Samples	T_{onset}	T_{50}	T_{max}
PLA	274.3	339.2	345.1
PLA/rGO	304.9	349.7	353.7
PLA/EPO/rGO	341.3	384.7	388.3
PLA/PEG/rGO	217.3	311.0	321.1
PLA/xGnP	297.3	339.7	347.9
PLA/EPO/xGnP	337.5	381.7	386.6
PLA/PEG/xGnP	201.1	296.6	307.5

From Figure 8, a slight improvement in thermal stability for all rGO nanocomposites can be observed. For the PLA/rGO, the half decomposition temperature (T_{50}) and maximum decomposition temperature (T_{max}) shifted up of about 10 °C and 6 °C as compared to nanocomposite with xGnP. Whereas, PLA/PEG/rGO showed improvement of 16 °C, 15 °C and 14 °C in T_{onset}, T_{50} and T_{max}, respectively. The enhanced thermal stability of the nanocomposites was attributed to the very high aspect ratio of rGO, which prevented the emission of small gaseous molecules during thermal degradation. The homogeneously dispersed rGO also disrupted the oxygen supply by forming a charred layer on the surfaces of the nanocomposites [31]. This indicates that rGO can act as a considerably good barrier to prevent the thermal degradation of PLA compared to that of xGnP.

3.5. Scanning Electron Microscopy (SEM)

The fracture surfaces of the pristine PLA, xGnP and rGO nanocomposites were examined by scanning electron microscope to study the morphology of the surface. Figure 9 shows SEM micrographs of fracture surface of PLA and both xGnP and rGO nanocoposites at magnification of 500×.

Figure 9. SEM images of (**a**) PLA; (**b**) PLA/xGnP; (**c**) PLA/rGO; (**d**) PLA/EPO/xGnP; (**e**) PLA/EPO/rGO; (**f**) PLA/PEG/xGnP; and (**g**) PLA/PEG/rGO.

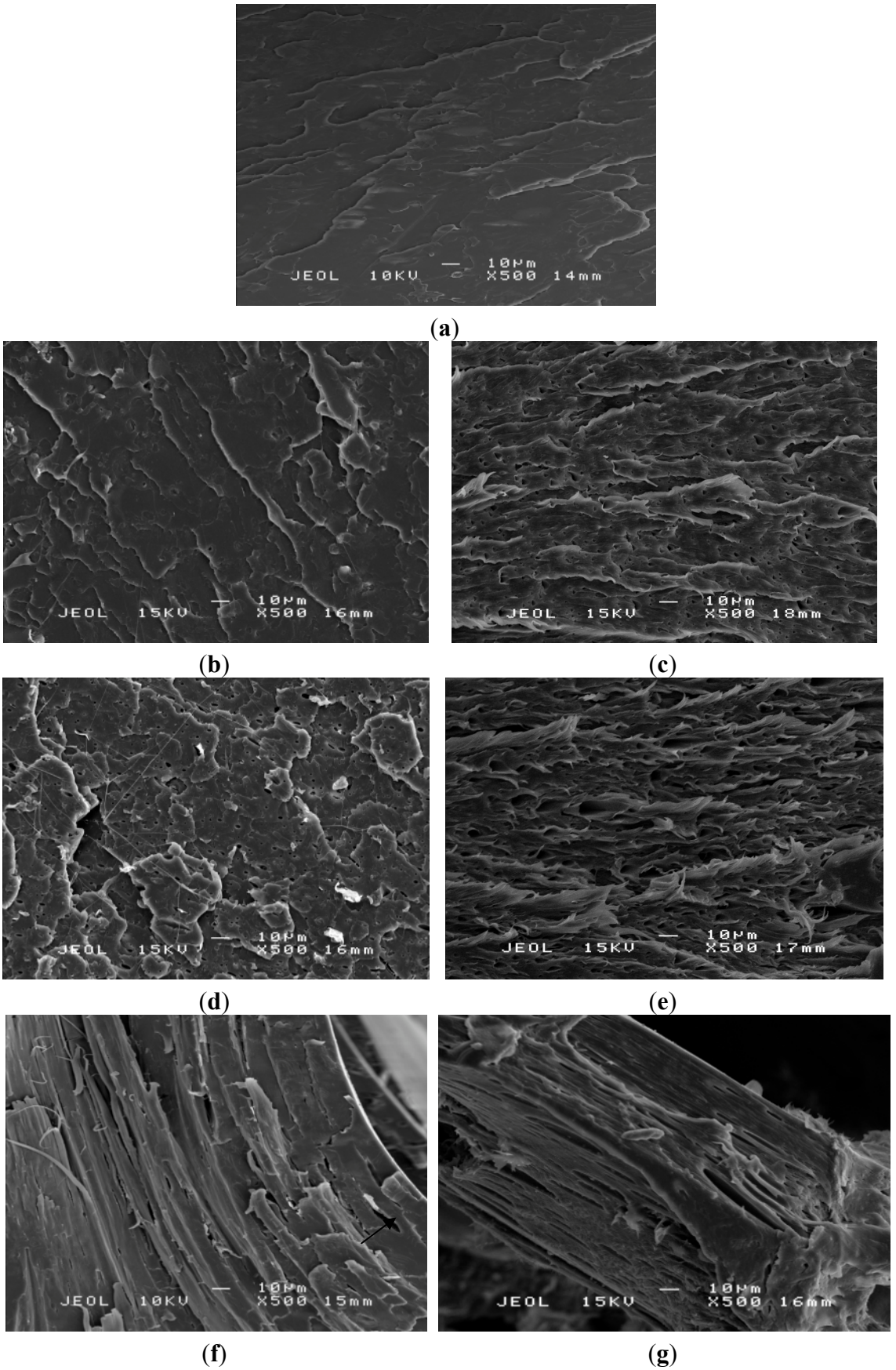

(**a**)

(**b**) (**c**)

(**d**) (**e**)

(**f**) (**g**)

As can be observed in Figure 9a, PLA shows a very clean and smooth fracture surface due to its brittle behavior at room temperature. The rGO nanocomposites display homogenous and good uniformity fracture surface. Good uniformity of composites indicates good degree of dispersion of the nanofiller and therefore results in better tensile strength. All the rGO nanocomposites exhibit a strong stretching effect conforming to the improved elongation at break during tensile testing, especially PLA/PEG/rGO, which give the highest elongation at break value of 531.9%. The SEM images of the nanocomposites agreed with the tensile results.

3.6. Transmission Electron Microscopy (TEM)

The performance of nanocomposites depends on dispersion of the nanofillers. TEM is a widely used technique to evaluate the dispersion of nano-additives in a polymer matrix. Thus, TEM micrographs were collected to gain better understanding of xGnP and rGO nanofiller dispersion. The TEM micrographs of PLA/rGO, PLA/EPO/rGO, and PLA/PEG/rGO are shown in Figure 10b,d,f respectively, which revealed that the rGO remained intact as graphene sheet layer and were dispersed into the polymer matrix. Meanwhile, TEM images of xGnP nanocomposites reveal that the xGnPs maintained the inherent layered structure after being blended with PLA, and some aggregation or agglomeration was observed, as shown in Figure 10a,c,e.

Figure 10. TEM images of (**a**) PLA/xGnP; (**b**) PLA/rGO; (**c**) PLA/EPO/xGnP; (**d**) PLA/EPO/rGO; (**e**) PLA/PEG/xGnP; and (**f**) PLA/PEG/rGO.

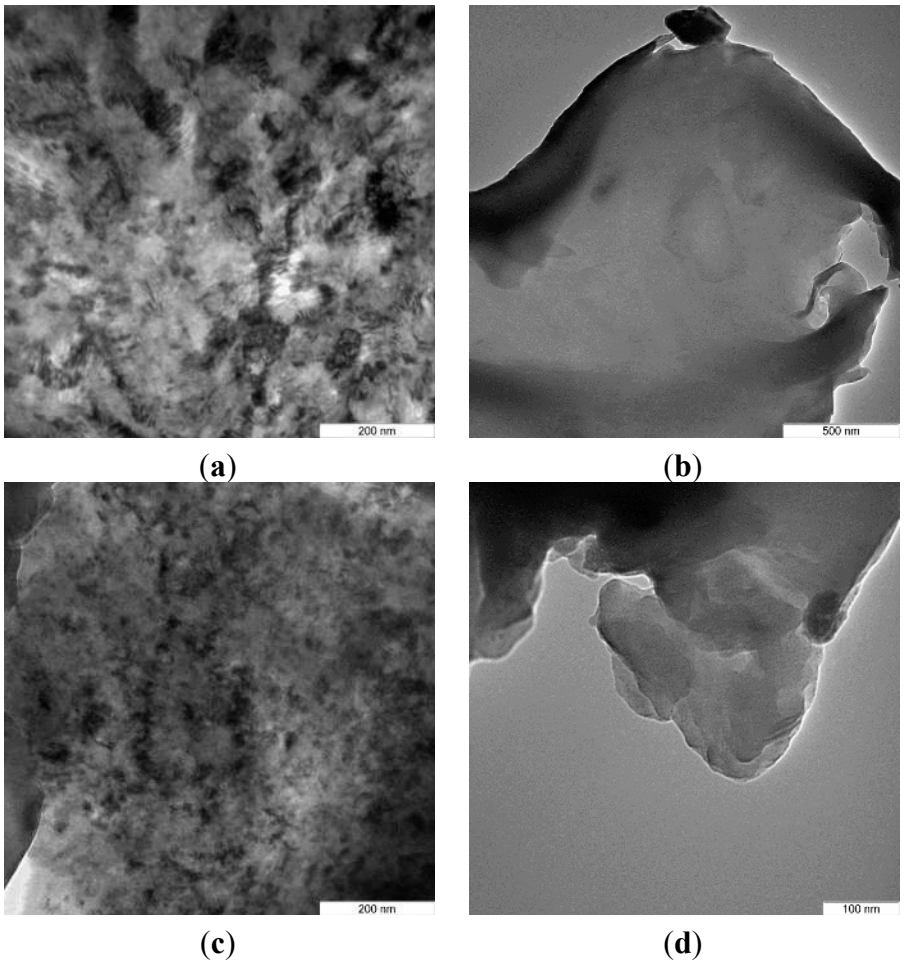

(**a**) (**b**)

(**c**) (**d**)

Figure 10. *Cont.*

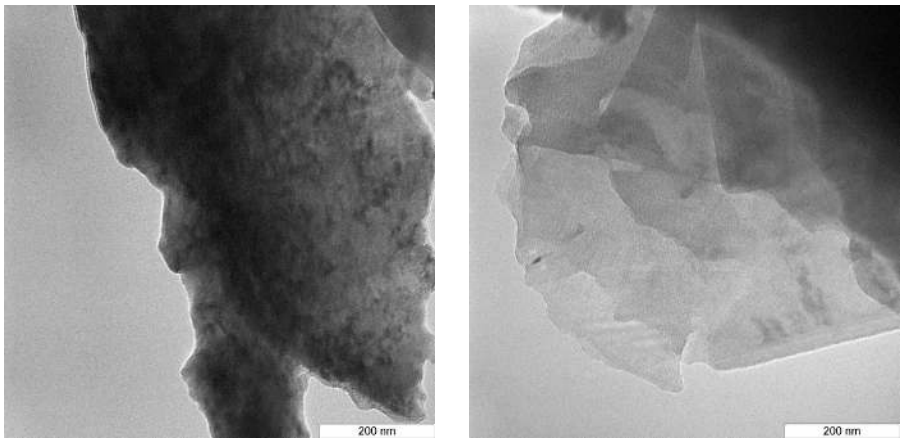

(e) **(f)**

4. Conclusions

Addition of rGO into PLA or plasticized PLA substantially enhanced the tensile strength without deteriorating elasticity, compared to xGnP nanocomposites. In addition, the investigation of the thermal properties by means of TGA has found that the presence of rGO in the system is very beneficial for improving thermal stability of the PLA or plasticized PLA. SEM images of the rGO nanocomposites display homogenous and good uniformity fracture surface. TEM images revealed that the rGO remained intact as graphene sheet layers and were dispersed well into the polymer matrix, and it was confirmed by the XRD result, which shows no graphitic peak in the XRD patterns. All these findings pointed out that the rGO is promising nanofiller to yield high performance nanocomposites compared to xGnP.

Acknowledgments

The authors would like to thank the Exploratory Research Grant Scheme (ERGS/1/11/STG/UPM/02/5) from Ministry of Higher Education (MOHE), Malaysia for their financial support.

Author Contributions

The first author was responsible for designing the research project and writing the journal article. The co-authors contributed in analysis of data, interpretation of the research finding and editing of this article.

Conflicts of Interest

The authors declare no conflict of interest.

References

1. Geim, A.K. Graphene: Status and prospects. *Science* **2009**, *324*, 1530–1534.
2. Kalaitzidou, K.; Fukushima, H.; Drzal, L.T. Mechanical properties and morphological characterization of exfoliated graphite-polypropylene nanocomposites. *Compos. A Appl. Sci. Manuf.* **2007**, *38*, 1675–1682.

3. Dreyer, D.R.; Jarvis, K.A.; Ferreira, P.J.; Bielawski, C.W. Graphite oxide as a carbocatalyst for the preparation of fullerene-reinforced polyester and polyamide nanocomposites. *Polym. Chem.* **2012**, *3*, 757–766.
4. Dreyer, D.R.; Jarvis, K.A.; Ferreira, P.J.; Bielawski, C.W. Graphite oxide as a dehydrative polymerization catalyst: A one-step synthesis of carbon-reinforced poly(phenylene methylene) composites. *Macromolecules* **2011**, *44*, 7659–7667.
5. Raquez, J.-M.; Habibi, Y.; Murariu, M.; Dubois, P. Polylactide (PLA)-based nanocomposites. *Prog. Polym. Sci.* **2013**, *38*, 1504–1542.
6. Notta-Cuvier, D.; Odent, J.; Delille, R.; Murariu, M.; Lauro, F.; Raquez, J.M.; Bennani, B.; Dubois, P. Tailoring polylactide (PLA) properties for automotive applications: Effect of addition of designed additives on main mechanical properties. *Polym. Test.* **2014**, *36*, 1–9.
7. Chieng, B.W.; Ibrahim, N.A.; Yunus, W.M.Z.W.; Hussein, M.Z. Poly(lactic acid)/Poly(ethylene glycol) polymer nanocomposites: Effects of graphene nanoplatelets. *Polymers* **2014**, *6*, 93–104.
8. Silverajah, V.S.G.; Ibrahim, N.A.; Yunus, W.M.Z.W.; Hassan, H.A.; Chieng, B.W. A comparative study on the mechanical, thermal and morphological characterization of poly(lactic acid)/epoxidized palm oil blend. *Int. J. Mol. Sci.* **2012**, *13*, 5878–5898.
9. Chieng, B.W.; Ibrahim, N.A.; Yunus, W.M.Z.W.; Hussein, M.Z. Plasticized poly(lactic acid) with low molecular weight poly(ethylene glycol): Mechanical, thermal, and morphology properties. *J. Appl. Polym. Sci.* **2013**, *130*, 4576–4580.
10. Chieng, B.W.; Ibrahim, N.A.; Yunus, W.M.Z.W.; Hussein, M.Z.; Silverajah, V.S.G. Graphene nanoplatelets as novel reinforcement filler in poly(lactic acid)/epoxidized palm oil green nanocomposites: Mechanical properties. *Int. J. Mol. Sci.* **2012**, *13*, 10920–10934.
11. Chieng, B.W.; Ibrahim, N.A.; Yunus, W.M.Z.W. Optimization of tensile strength of poly(lactic acid)/graphene nanocomposites using response surface methodology. *Polym. Plast. Technol. Eng.* **2012**, *51*, 791–799.
12. Gumus, S.; Ozkoc, G.; Aytac, A. Plasticized and unplasticized PLA/organoclay nanocomposites: Short- and long-term thermal properties, morphology, and nonisothermal crystallization behavior. *J. Appl. Polym. Sci.* **2011**, *123*, 2837–2848.
13. Wu, C.-S.; Liao, H.-T. Study on the preparation and characterization of biodegradable polylactide/multi-walled carbon nanotubes nanocomposites. *Polymer* **2007**, *48*, 4449–4458.
14. Chiang, M.-F.; Wu, T.-M. Synthesis and characterization of biodegradable poly(L-lactide)/layered double hydroxide nanocomposites. *Compos. Sci. Technol.* **2010**, *70*, 110–115.
15. Zhang, Y.Y.; Gu, Y.T. Mechanical properties of graphene: Effects of layer number, temperature and isotope. *Comput. Mater. Sci.* **2013**, *71*, 197–200.
16. Via, M.D.; King, J.A.; Keith, J.M.; Miskioglu, I.; Cieslinski, M.J.; Anderson, J.J.; Bogucki, G.R. Tensile modulus modeling of carbon black/polycarbonate, carbon nanotube/polycarbonate, and exfoliated graphite nanoplatelet/polycarbonate composites. *J. Appl. Polym. Sci.* **2012**, *124*, 2269–2277.
17. Xu, Z.; Gao, C. *In situ* polymerization approach to graphene-reinforced nylon-6 composites. *Macromolecules* **2010**, *43*, 6716–6723.
18. Huang, Y.; Wang, X.; Jin, X.; Wang, T. Study on the PMMA/GO nanocomposites with good thermal stability prepared by *in situ* Pickering emulsion polymerization. *J. Therm. Anal. Calorim.* **2014**, *117*, 755–763.

19. Chandrasekaran, S.; Seidel, C.; Schulte, K. Preparation and characterization of graphite nano-platelet (GNP)/epoxy nano-composite: Mechanical, electrical and thermal properties. *Eur. Polym. J.* **2013**, *49*, 3878–3888.
20. Wang, J.; Wang, X.; Xu, C.; Zhang, M.; Shang, X. Preparation of graphene/poly(vinyl alcohol) nanocomposites with enhanced mechanical properties and water resistance. *Polym. Int.* **2011**, *60*, 816–822.
21. Oxfall, H.; Rondin, J.; Bouquey, M.; Muller, R.; Rigdahl, M.; Rychwalski, R.W. Elongational flow mixing for manufacturing of graphite nanoplatelet/polystyrene composites. *J. Appl. Polym. Sci.* **2013**, *128*, 2679–2686.
22. Haghighi, A.; Sheydaei, M.; Allahbakhsh, A.; Ghatarband, M.; Hosseini, F. Thermal performance of poly(ethylene disulfide)/expanded graphite nanocomposites. *J. Therm. Anal. Calorim.* **2014**, *117*, 525–535.
23. Xu, Y.; Chen, M.; Ning, X.; Chen, X.; Sun, Z.; Ma, Y.; Yu, J.; Zhang, Z.; Bo, X.; Yang, L.; *et al*. Influences of coupling agent on thermal properties, flammability and mechanical properties of polypropylene/thermoplastic polyurethanes composites filled with expanded graphite. *J. Therm. Anal. Calorim.* **2014**, *115*, 689–695.
24. Cao, Y.; Feng, J.; Wu, P. Preparation of organically dispersible graphene nanosheet powders through a lyophilization method and their poly(lactic acid) composites. *Carbon* **2010**, *48*, 3834–3839.
25. Pinto, A.M.; Cabral, J.; Tanaka, D.A.P.; Mendes, A.M.; Magalhães, F.D. Effect of incorporation of graphene oxide and graphene nanoplatelets on mechanical and gas permeability properties of poly(lactic acid) films. *Polym. Int.* **2013**, *62*, 33–40.
26. Rafiee, M.A.; Rafiee, J.; Wang, Z.; Song, H.; Yu, Z.-Z.; Koratkar, N. Enhanced mechanical properties of nanocomposites at low graphene content. *ACS Nano* **2009**, *3*, 3884–3890.
27. Inuwa, I.M.; Hassan, A.; Samsudin, S.A.; Mohamad Kassim, M.H.; Jawaid, M. Mechanical and thermal properties of exfoliated graphite nanoplatelets reinforced polyethylene terephthalate/polypropylene composites. *Polym. Compos.* **2014**, *2014*, doi:10.1002/pc.22863.
28. *Standard Test Method for Tensile Properties of Plastics*; ASTM D638-10; ASTM (American Society for Testing and Materials) International: West Conshohocken, PA, USA, 2010.
29. Li, W.; Xu, Z.; Chen, L.; Shan, M.; Tian, X.; Yang, C.; Lv, H.; Qian, X. A facile method to produce graphene oxide-g-poly(L-lactic acid) as an promising reinforcement for PLLA nanocomposites. *Chem. Eng. J.* **2014**, *237*, 291–299.
30. Daniels, P.H. A brief overview of theories of PVC plasticization and methods used to evaluate PVC-plasticizer interaction. *J. Vinyl Addit. Technol.* **2009**, *15*, 219–223.
31. Kuila, T.; Bose, S.; Mishra, A.K.; Khanra, P.; Kim, N.H.; Lee, J.H. Effect of functionalized graphene on the physical properties of linear low density polyethylene nanocomposites. *Polym. Test.* **2012**, *31*, 31–38.